Case Studies in Thermal Engineering 8 (2016) 176–186

Contents lists available at ScienceDirect

Case Studies in Thermal Engineering

journal homepage: www.elsevier.com/locate/csite

A linear Fresnel reflector as a solar system for heating water: Theoretical and experimental study

Ghodbane Mokhtar [a,*], Boumeddane Boussad [a], Said Noureddine [b]

[a] Faculty of Technology, Mechanical Department, University of Blida 1, Algeria
[b] CSP, Alger, Algeria

ARTICLE INFO

Article history:
Received 4 April 2016
Received in revised form
17 June 2016
Accepted 19 June 2016
Available online 5 July 2016

Keywords:
Linear Fresnel receiver
Thermal energy
Thermal efficiencies
Solar water heating system

ABSTRACT

This work is concerned with assessing the thermal performances of a solar water heating system which is dependent on a linear Fresnel receiver (LFR) as a solar energy converter. The main objective of this paper is validation the experimental work carried out in the winter of 2015 on the concentrator in the climatic conditions of Algerian city "Blida" by a numerical simulation, where the tap water used as a heat carrier fluid. This simulation was used to solution of the energy balance equations of the absorber tubes and the water, where the solution is based on the finite difference method with an implicit scheme. After the solution of nonlinear equations, the program performed by using the MATLAB language gives the thermal efficiencies, the absorber temperatures, the water temperatures at the absorber tubes outlet, and thermal losses coefficients. The thermal efficiency of the reflector is exceeded 29%. The results obtained proved the existence of substantial convergence between the experimental and the numerical results, where in all cases the water temperature exceeded 347 K.
© 2016 The Authors. Published by Elsevier Ltd. This is an open access article under the CC BY-NC-ND license (http://creativecommons.org/licenses/by-nc-nd/4.0/).

1. Introduction

Fresnel collectors have two types: the linear Fresnel reflector (LFR) and the Fresnel lens collector (FLC) [1]. The linear Fresnel mirror concentrator technology is still young and has taken place in the field of concentrating solar systems, this technology was conceived by the French physicist Augustin-Jean FRESNEL (1788–1827), he was used this technique in the optical system of the marine indication headlights [2]. The work of Alessandro Battaglia is the origin of the concentration technique by linear Fresnel reflector [3,4]. The Italian mathematician Giovanni Francia (1911–1980), designed the first prototype of linear Fresnel concentrator with the downward facing aperture covered with glass honeycomb tubes at Marseille built in 1962, he got on the performance equal to 60% and steam water temperature equivalent to 450 °C [5]. In the general case and according to the literature searches, the performance of this type of concentrator is varied between 30% and 40% [6,7].

In this day of many international institutions are investing and working to develop this technology, for instance at Almeria in Spain, the German company NOVATEC BIOSOL built the first commercial linear Fresnel reflector plant in the world. This electric station has a capacity of 1.4 MW, and since March 2009, their power supplies the local electricity power lines [8]. In France and since August 2010, CNIM group invested the only module of its Linear Fresnel solar concentrator at

* Corresponding author.
E-mail address:

http://dx.doi.org/10.1016/j.csite.2016.06.006
2214-157X/© 2016 The Authors. Published by Elsevier Ltd. This is an open access article under the CC BY-NC-ND license (http://creativecommons.org/licenses/by-nc-nd/4.0/).

Nomenclature

ΔX	length element, m
$A_{A,\ ext}$	surface external of absorber, m^2
$A_{A,\ int}$	surface intern of absorber, m^2
A_c	total collector aperture area, m^2
C_A	specific heat of the absorber, J/kg K
C_F	specific heat of the fluid, J/kg K
$D_{A,\ ext}$	diameter external of absorber, m
$D_{A,\ int}$	diameter external of absorber, m
DNI	direct-normal irradiance, W/m^2
f	focal length, m
h_F	heat transfer coefficient by convection, W/m^2 K
h_w	wind heat transfer coefficient, W/m^2 K
j	number of day
K_F	thermal conductivity of the fluid, W/m^2 K
L	absorber tube length, m
L_m	mirror length, m
Nu	nusselt number
Pr	prandtl number
$q_{absorbed}$	thermal power received by the absorber tubes, W
q_{ext}	global heat exchange between the absorber and the environment, W
$q_{ext,\ conv}$	convection exchange between the absorber and the environment, W
$q_{ext,\ ray}$	radiation exchange between the absorber and the environment, W
q_{gain}	heat flux exchanged by convection between the cylindrical absorbent tubes and fluid, W
q_{out}	quantity of a heat to the output of an element of the absorber tubes, W
Q_V	volume flow of the water with the intern to absorber, m^3/s
Re	Reynolds number
S_e	reflectors effective surface, m^2
T_A	absorber temperature, K
T_{amb}	ambient temperature, K
T_F	fluid temperature, K
T_{fi}	water inside temperature, °C
T_{fo}	water outside temperature, °C
U_L	heat transfer loss coefficient of solar collector, W/m^2 K
V_w	wind speed, m/s
W	width of the mirror, m
ϕ	latitude, deg
ω	hour angle, deg

Greek symbols

α	absorption coefficient of the absorber tube
α_F	fluid thermal diffusivity, m^2/s
γ	interception factor
δ	declination angle, deg
ε_{Ab}	absorber emissivity
η	thermal efficiency
η_{opt}	optical efficiency
θ_n	slope angle of an nth mirror element, deg
θ_t	angle in the transversal plane, deg
μ	dynamic viscosity, kg/m s
ν	kinematic viscosity, m^2/s
ρ_A	absorber density, kg/m^3
ρ_F	fluid density, kg/m^3
ρ_m	reflectance factor of the mirror
σ	Stefan-Boltzmann constant, W/m^2 K^4

the site of Lagoubran to generate electricity from a steam turbine [8]. In Australia, the company Areva has developed the technology of a linear Fresnel concentrator for electricity generation, Australia has two central, the first is Kimberlina in Bakersfield, California with a rated power of 24 MW, the second central will be built in Kogan Creek near Dalby at Australia, where their capacity equal to 44 MW [8].

There are many studies, addressed to use of the technology of linear Fresnel reflector, including the study conducted by Choudhury et al. [9], they made a design and analysis of a linear Fresnel Reflector (LFR), where they got the concentration ratio of 18% with two-thirds of the periphery of a tubular receiver of 0.025 m in diameter, their concentration can produce temperatures above 350 °C. Singh et al. [10], who studied the performance of the linear Fresnel solar concentration device with a single absorber tube of an aluminum which contains Hytherm-500 oil as heat carrier fluid. Mills et al. [11], they evaluated concept of a compact linear Fresnel (CLFR), assuming that the size of the solar field will be great, because it must be designed for the production of electricity across MW. In the field of water heating in the range between 60 and 95 °C, Singh et al. [10], studied the thermal performance of the linear Fresnel concentrator which contains a trapezoidal cavity with two types of absorber tubes (rectangular and circular). The reflector performance of their collectors is varied between 16% and 64%, depending on the shape of the absorber tubes and the quality of the selective surface [12]. Moghimi et al. used the Computational Fluid Dynamics (CFD) to estimate the optical efficiency of linear Fresnel reflector, their study is considered a new or innovative computational approach for an accurate assessment of the contributions of heat loss in a multi-tube trapezoidal cavity receiver [13]. In another study, Moghimi et al. conducted a mathematical optimization on the trapezoidal cavity absorber for the Linear Fresnel Reflector In order to get the optimal designs of the cavity, the objectives of their study are finding the most appropriate architecture to reduce heat losses and side wind load [14].

The water-heaters are an essential instrument in our daily lives; it use of large-scale domestically and industrially. There are many scientific research conducted on solar water-heaters, which it has been used several types of solar collector [15–19]. This paper aims to characterize the thermal performances of a solar system for heating water which is based on a linear Fresnel solar converter in the city of Blida, Algeria. The thermal study was made by numerical simulation; this simulation is

Fig. 1. Scheme of the experimental device.

developed by the MATLAB programming language according to equations of energy balance (fluid and absorber tubes). This thermal modeling enabled us to calculate each of: the thermal efficiencies, the absorber temperatures, the water temperatures at outlet of absorber tubes and the thermal losses coefficients. The numerical results were compared with the experimental results which conducted in the winter of 2015.

2. Thermal modeling

The solar reflector adopted in this study is a linear Fresnel concentrator; this solar concentrator has been designed and installed at the Mechanics department of SAAD DAHLAB University_ Blida 1, at Algeria. Fig. 1 presents a prototype of a linear Fresnel reflector with a full surface of reflecting mirrors equal to 1.65 m^2.

The solar reflector (Fig. 1) is composed of five elements, they are as follows:

- *Exterior support frame:* it's used to support the weight of the horizontal base with its reflecting mirrors and the absorber tubes with all its components. It is made of four angle section metal bars (Length = 1760 mm, Width = 30 mm, Height = 30 mm and thickness = 02 mm).
- *Interior support frame:* it's one of the most important components in this device because it bears the reflecting mirrors. It is consisted of four hollow square metal bars (Length = 1600 mm, Width = 30 mm, Height = 30 mm and Thickness = 1 mm).
- *Reflecting mirrors:* the experimental device contains eleven reflective mirrors strips (1500 mm × 100 mm) to redirect and concentrate the direct solar radiation towards a fixed absorber tubes.
- *Trapezoidal cavity:* the trapezoidal cavity is a folded galvanized sheet (Length = 2000 mm, Width = 1000 mm and thickness = 1.5 mm) in the form of (U). The vacuum inside it was filled with polystyrene (Length = 3000 mm, Width = 1000 mm and thickness = 100 mm). The white Formica plates (Length = 1700 mm, Width 1 = 100 mm, Width 2 = 125 mm and thickness = 4 mm) was glued on polystyrene with silicone and double-sided sellotape. The all gave us a trapezoidal shape. Fig. 2 presents the dimensions of trapezoidal cavity with the four absorber tubes.
- *Absorber tubes:* they are made of a copper pipe (Ø20/22 mm and length (L) equal to 1600 mm) and placed in the cavity, there are four tubes; they are plated with painted black and covered by selective suitable surface. The selective layer was used on the absorber to increase its operation temperature and efficiencies [20].

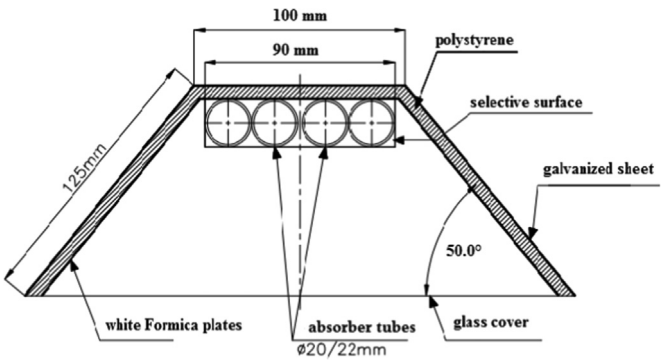

Fig. 2. Geometric shape of the trapezoidal cavity geometry.

Table 1
Dimensional geometric of the solar collector.

Element	Value	Unity
External diameter of the absorber ($D_{A,\ ext}$)	22	mm
Internal diameter of the absorber ($D_{A,\ int}$)	20	mm
Mirror length (L_m)	1500	mm
Mirror width (W)	100	mm

Table 1 includes the geometric parameters of the collector.

The optical parameters of the collector are illustrated in Table 2.

Fig. 3 illustrates the mirrors configuration at 12:00.

Table 3 includes the configuration of each mirror according to the geometric parameters of our prototype at 12:00. These configurations account from the equations mentioned in the both articles of Singh et al. [10,12], the focal distance (f) between the absorber tubes and the central mirror equal to 1300 mm.

The absorber tubes are made of Copper covered with an adapted a selective coating; they are placed along the focal line of the linear Fresnel concentrator. The heat exchange existing in the system takes place between the heat transfer fluid and the absorber tubes.

These the several simplifying assumptions were used during the calculation:

- The fluid flow is one-dimensional.
- The all properties of the fluid (water) depend on the temperature.
- The temporal variation in the thickness of the absorber tubes is negligible.
- The exchange by conduction in the absorber is negligible.
- The thermal flux is uniformly distributed on the level of the absorber tubes.

Fig. 4 demonstrates the various forms of heat exchanges which take place in the absorber tubes and environment around him.

2.1. Heat exchange between the absorber and the fluid

The temperature modeling is based on the energy balances, which are characterized by the differential equations of fluid temperatures (T_F) and absorber temperature (T_A). Eq. (1) presents the thermal power emitted by the sun and received by absorber tubes [21,22].

$$q_{absorbed} = 0.7\ \alpha\ \rho_m\ \gamma\ S_e\ DNI\ \sqrt{1 - \cos^2(\delta)\sin^2(h)} \tag{1}$$

Factor α is the absorption coefficient of the absorber tubes, ρm is the reflectance factor of the mirror, γ is the interception factor and DNI is the direct solar radiation, δ is declination angle, h is the sun altitude.

The declination angle (δ) is the angle between the terrestrial equator planes and the earth-sun direction. This angle varies throughout the year symmetrically of −23°26′ to 23°26′ [23]. The declination (δ) is the point's latitude of the earth which are achieved by the midday sun (noon-solar), it is directly related to the number of day (j) of the year as it turns out in the Eq. (2) [24].

$$\delta = 23,45^\circ \sin[0,980^\circ (j + 284)] \tag{2}$$

But the height of the sun (h) is the angle that the sun direction with its projection on the ground, it varies from 0° to 90° in the southern hemisphere (Nadir), vanishes at sunrise and sunset and is maximal in the south-solar. It's in term of the latitude (ϕ) and the hour angle (ω).

$$h = \arcsin(\cos\varphi \cos\delta \cos\omega + \sin\varphi \sin\delta) \tag{3}$$

S_e is the effective surface of mirror aperture; this surface can calculate by the following equation [25]:

Table 2
Optical properties of materials used.

Properties	Value
Absorption coefficient of absorber tubes, α	0.8
Surface reflectance of the mirror, ρ_m	0.85
Emissivity of absorber tube, ε_A	0.12

Fig. 3. The configuration of mirrors at 12:00.

Table 3
Mirrors configuration according to the geometric parameters of the concentrator (LFR).

n	Position (Q) (mm)	Distance between the mirrors (S) (mm)	Inclination (θ) (deg)
0 (Central mirror)	0	0	0
1 et 6	50	0	2.528
2 et 7	150	0	5.337
3 et 8	250.8	0.8525	8.065
4 et 9	353.1	2.737	10.69
5 et 10	457.7	5.566	13.18

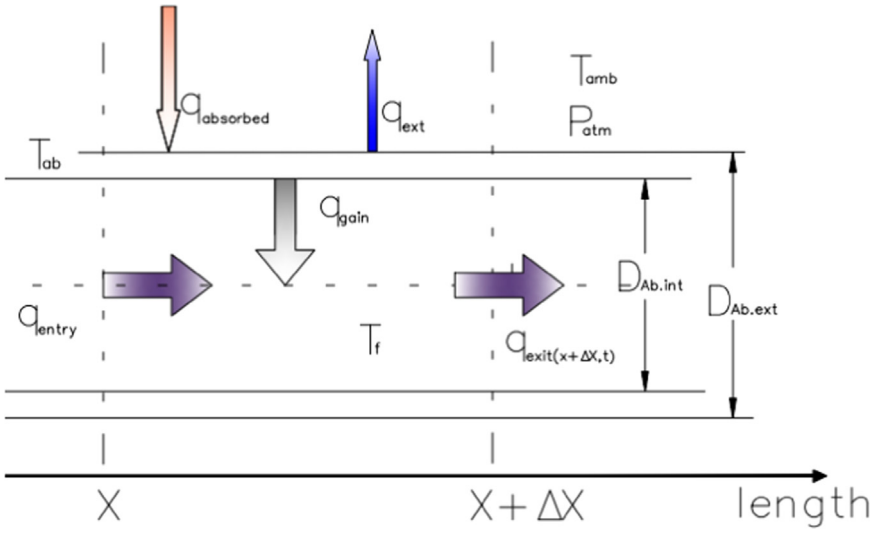

Fig. 4. Energy balance on the level of the absorber tube.

$$S_e = \sum_{n=1}^{k} W.\cos(\theta_t - \theta_n) \tag{4}$$

Where W is the mirror width, θ_t is the angle in the transversal plane and θ_n is the slope angle of an nth mirror element.

Eq. (5) enables us to calculate the heat flux exchanged by convection between the cylindrical absorbent tubes and fluid (water).

$$q_{gain} = h_F A_{A,\,int} (T_A - T_F) \tag{5}$$

It was observed that Eq. (5) associated with the coefficient of heat exchange by convection (h_F), this coefficient related to the mode of fluid flow. So, h_F given by the following expression:

$$h_F = \frac{Nu \times K_F}{D_{A,\,int}} \tag{6}$$

Where K_F presents the thermal conductivity of the fluid.

In this study the flow regime of the water is laminar ($Re < 2300$), the Nusselt Number (Nu) in type of flow is given by [22,26,27]:

$$Nu = 3.66 + \frac{0.0668 Re_F Pr \frac{D_{A,\,int}}{L}}{1 + 0.04\left(Re_F Pr \frac{D_{A,\,int}}{L}\right)^{\frac{2}{3}}} \tag{7}$$

The factor (Re_F) presents Reynolds number which is expressed by the following relation [28]:

$$Re_F = \frac{4 \times \rho_F \times Q_V}{\pi \times D_{A,\,int} \times \mu_F} \tag{8}$$

With μ_F which indicates the dynamic viscosity of the fluid, where the analogy of Reynolds number is established by the intimate bond viscosity phenomena and heat transfer.

The Prandtl number (Pr) will be written in the following form [29]:

$$Pr_F = \frac{\nu_F}{\alpha_F} \tag{9}$$

ν_F is the kinematic viscosity, it's defined by [30]:

$$\nu_F = \frac{\mu_F}{\rho_F} \tag{10}$$

The fluid thermal diffusivity (α_F) is defined by [31]:

$$\alpha_F = \frac{K_F}{\rho_F \times C_F} \tag{11}$$

The energy balance for the heat transfer fluid circulating in the absorber tubes is expressed by the following relationship:

$$\rho_F \times C_F \times \pi \times D_{A,\,int} \frac{\partial T_F(X,\,t)}{\partial t} = q_{gain} - \rho_F \times C_F \times Q_V \frac{\partial T_F(X,\,t)}{\partial X} \tag{12}$$

The initial conditions and boundary conditions of Eq. (12) are:

$$\begin{cases} T_F(0,\,t) = T_{F,inlet}(t) = T_{amb}(t) \\ T_F(X,\,0) = T_{F,initial}(t) = T_{amb}(0) \end{cases} \tag{13}$$

2.2. Heat exchange between the absorber and the ambient

The energy balance for the absorber tube is given by the following equation:

$$\rho_A \times C_A \times \pi \times (D_{A,ext} - D_{A,\,int}) \frac{\partial T_F(X,\,t)}{\partial t} = q_{absorbed}(t) - q_{out}(X,\,t) - q_{gain}(X,\,t) \tag{14}$$

With, (q_{out}) is the heat quantity at the output of the absorber tube element.

$$q_{out}(X + \Delta X,\,t) = \rho_F \times C_F \times Q_V \times \Delta X \times T_F(X + \Delta X,\,t) \tag{15}$$

Eq. (16) presents the initial conditions of Eq. (15).

$$T_A(X,\,0) = T_{A,initial}(t) = T_{amb}(0) \tag{16}$$

Eq. (17) illustrated the global heat exchange between the absorber and the environment.

$$q_{ext} = q_{ext,conv} + q_{ext,ray} \tag{17}$$

The convection exchange between the absorber and the environment ($q_{ext,\,conv}$) can account by using Eq. (18).

$$q_{ext,conv} = h_w A_{A,ext} (T_A - T_{amb}) \tag{18}$$

According to McAdams (1954) [22], the heat transfer coefficient of wind (h_w) is given by:

$$h_w = 5.7 + 3.8\,V_w \tag{19}$$

The radiation exchange between the absorber tubes and the environment ($q_{ext,\ ray}$) can calculate by Eq. (20).

$$q_{ext,ray} = \varepsilon_A\,\sigma\,A_{A,ext}\,(T_A^4 - T_{amb}^4) \tag{20}$$

For the analysis and dissemination of equations, the finites differences method was used to discretize the principal equations of the phenomenon. Eq. (21) and Eq. (22) present the equations of the unknowns (T_A) and (T_F) after deployment and analysis of the previous equations.

$$T_{F,j}(t) = -\frac{Q_V}{\pi \times D_{A,\ int} \times \Delta X}T_{F,j}(t) + \frac{\left(\rho_F \times C_F\right)_{\Pi_{F,j-1}} \times Q_V}{\left(\rho_F \times C_F\right)_{\Pi_{F,j}} \times \pi \times D_{A,\ int} \times \Delta X}T_{F,j-1}(t) + \frac{1}{\left(\rho_F \times C_F\right)_{\Pi_{F,j}} \times \pi \times D_{A,\ int} \times \Delta X}h_F \times \pi \times D_{A,\ int}(T_{A,j} - T_{F,j}) \tag{21}$$

$$T_{A,j}(t) = -\frac{Q_V}{\pi(D_{A,ext} - D_{A,\ int})}(q_{absorbed}(t) - h_w \times \pi \times D_{A,ext}(T_{A,j}(t) - T_{amb}(t)) - \varepsilon_A \times \sigma \times \pi \times D_{A,ext}(T_{A,j}^4(t) - T_{amb}^4(t)) - h_F \times \pi \times D_{A,\ int}(T_{A,j}(t) - T_{F,j}(t))) \tag{22}$$

To solve this system reformulates of all relations, (Eqs. (21) and 22) can be written in the form of a matrix as follows: [A].[T]=[B], where [A] represents the coefficient matrix, [T] is the vector of unknowns and [B] is the vector of the second member (B is not null). The method of Gauss-Seidel with total pivot was adapted for the resolution of this system, because this method converges rapidly and removes the matrix inversion.

2.3. The thermal losses coefficient

Solar energy which descends on the absorber tubes is not entirely transmitted to the fluid; a part is dissipated in the form of thermal losses between the absorber and ambient air. The thermal loss coefficient is given by the following relation [32]:

$$U_L = \varepsilon_A\,\sigma\,(T_A^2 + T_{amb}^2)(T_A + T_{amb}) \tag{23}$$

With (σ) is Stefan-Boltzmann constant (σ=5.66897 10^{-8} W/m^2 K^4).

2.4. Thermal efficiency

The thermal efficiencies of our concentrator are given by the following equation [32]:

$$\eta = \eta_{opt} - \frac{U_L A_{A,ext}(T_A - T_{amb})}{DNI \times A_C} \tag{24}$$

Where η_{opt} is the optical efficiencies of the collector (LFR), it can be calculated by Eq. (25) [33].

$$\eta_{opt} = 0.7\,\alpha\,\rho_m\,\gamma\,\sqrt{1 - \cos^2(\delta)\sin^2(h)} \tag{25}$$

3. Results and discussion

Algeria is among the countries that have great potential solar energy in the world [27,34–36]. Blida is one of the Algerian cities; this site was chosen to conduct our experiment work. The geographic coordinates of Blida are altitude=260 m, its latitude=36°28′N and its longitude=2°49′E. Two types of the relief characterize Blida; the first is the Mitidja plain with fertile land and its very low slopes; the second is the zone of the Blidian Atlas and piedmont. The average annual temperature is fairly stable; it is about 11.5 °C in winter and 33 °C in summer. The average annual rainfall is about 600 mm, it is more important in the Atlas. The dominant winds in Blida city are the wind from the east and west, and the sirocco in summer. Fig. 5 presents the variation of the direct-normal irradiance (DNI) depending on time for the two days of the manipulation (January 22nd and February 19th, 2015).

Polynomial equations of the direct solar radiation (DNI) for the days in term of the time (t) are:

- January 22nd, 2015

$$DNI = -3039.21429 + 635.96429 \times t - 26.75 \times t^2 \tag{26}$$

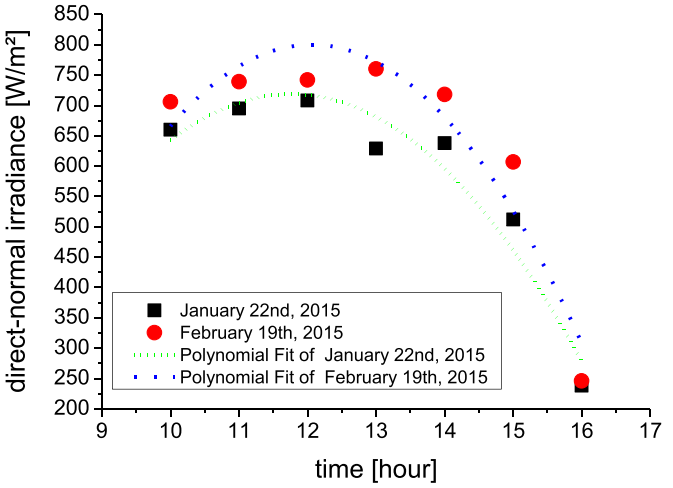

Fig. 5. Recorded direct solar radiation during the testing days.

- February 19th, 2015

$$DNI = -3831.5 + 765.69048 \times t - 31.66667 \times t^2 \quad (27)$$

Through the Fig. 5, it is obvious to note that the maximum direct solar radiation value registered on 19 February at 13:00, where is reached 760 W/m^2. During the experiments, some clouds were observed, specifically between 12:00 o′clock and 14:00 o′clock for the 22nd January. In general, the direct solar radiation increases from sunrise to reach the maximum in the middle of the day and then it is back down in the evening. So, the use of solar energy is well-suited of our applications that need to coincide with the sunniest hours a day.

The optical efficiency (η_{opt}) of our concentrator is 29.5%. The water flow during the experiments and during the simulation is equal to 0.015 kg/s. The water temperature (T_{fi}) at inlet of the absorber tubes is equal to 12 °C. Table 4 includes the summary of the maximum values of the thermal efficiencies for our concentrator.

After the maximum values, the efficiency is decreased because the high quantity of the thermal loss. This loss is resulting from the rising absorber tubes temperature and ambient air temperature at the same time. There is a convergent gap between the experimental and numerical performance, this means that the good orientation of the solar concentrator mirrors towards the sun during the manipulation. Therefore, our device has a better efficiency in cold weather conditions.

In this section, it is presented the comparison curves between the experimental and numerical results. Fig. 6a-b illustrate the evolution of experimental and numerical results of absorber tubes temperature versus the time, but the Fig. 7a-b present the evaluation of experimental and numerical results of water temperature versus the time.

According to the Fig. 6a-b, the absorber tubes temperature increase with the start of the day until it reaches it maximum value, and then back down influenced by the lack of the quantity of direct solar radiation. The effect of clouds on January 22nd is very apparent on the results, the absorber tubes temperature (experimentally and numerically) dropped at 13:00. when the solar radiation on February 19th is stronger than January 22nd, this means the absorber tubes temperature on February 19th is greater than January 22nd.

Based on the Fig. 7a-b, similarity is noticed between the experimental and the numerical results, this means the good agreement between the numerical approaches and the experimental values. It is clear to see that the temperature variation depends in particular on the incident direct solar radiation and the surrounding climate of site. Table 5 includes the comparison between the maximum values of temperature (experimentally and numerically).

From the Figs. 6a-7b, the temperature depends mainly on the solar power received by absorber tubes; this absorbed power in term of concentrator geometrical characteristics, optical parameters, and direct solar radiation received by the collector. The water temperature (T_F) is lower than (T_A) for the two days, because the inner face of the absorber tubes absorbs the infrared radiation, which undergoes an increase in the temperature (T_A) (greenhouse effect). Consequently, the temperature of the external face is lower, because the winds create a convection phenomenon with the external side of the

Table 4
Maximum values of the thermal efficiencies.

The date	Maximum value of thermal efficiency	
	Numerical	Experimental
22/01/2015	0.29210466	0.29212
19/02/2015	0.29199905	0.29205

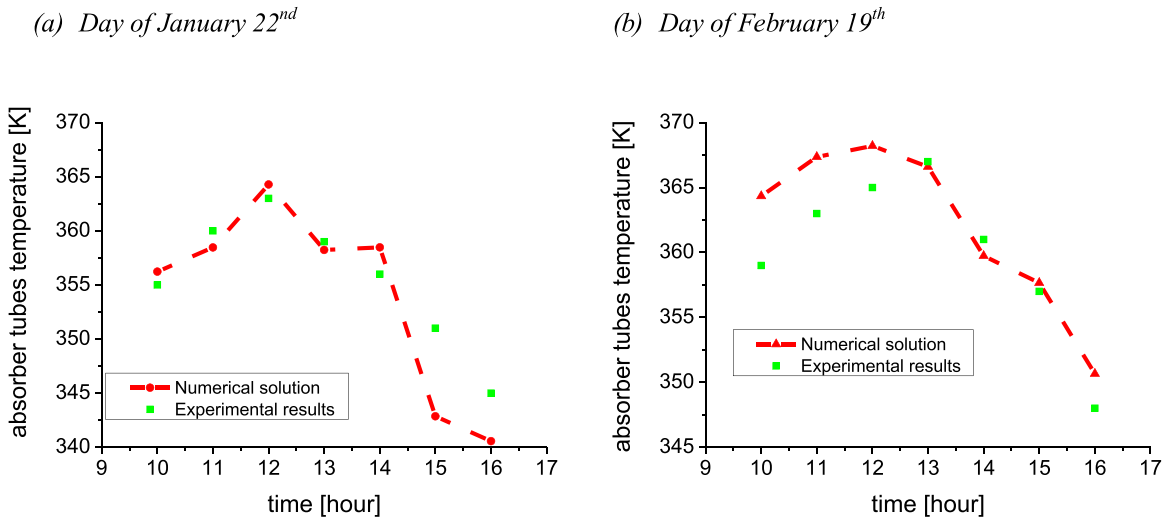

Fig. 6. Evolution of experimental and numerical temperature of the absorber tubes.

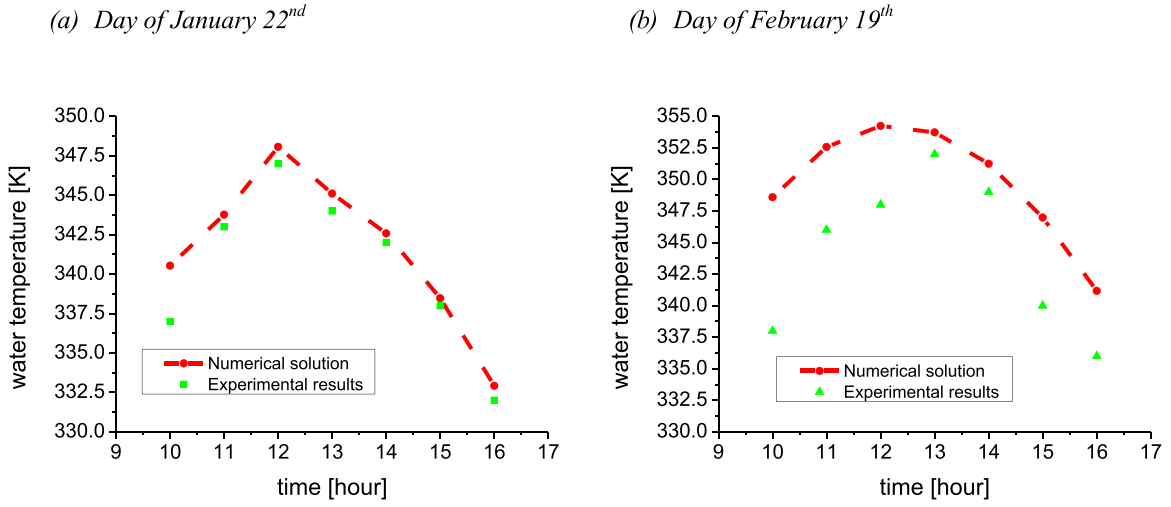

Fig. 7. Evolution of experimental and numerical temperature of the water.

Table 5
Maximum values of temperature.

Date	Absorber temperature (K)		Water exit temperature (K)	
	Numerical	Experimental	Numerical	Experimental
January 22nd	364.29	363	348.58	347
February 19th	367.31	367	354.25	352

absorber tubes.

The incidental solar energy absorbed by the absorber is not completely transmitted to the water in the form of heat; some quantity is dissipated as heat loss between the absorber tubes and the ambient air. This means that the heat loss coefficient (U_L) is an essential factor to determine the performance of our device, which when this factor is smaller, undoubtedly the efficiency of the concentrator would be better. Fig. 8a-b present the evaluation of the heat loss coefficient in terms of the difference between the absorber tubes temperature and the ambient air temperature.

The thermal efficiency decreases when the solar insolation increases, this decrease is due to thermal losses that believe with rising water temperatures respectively at the inlet and outlet of the absorber tube. So, the thermal losses increase rapidly when:

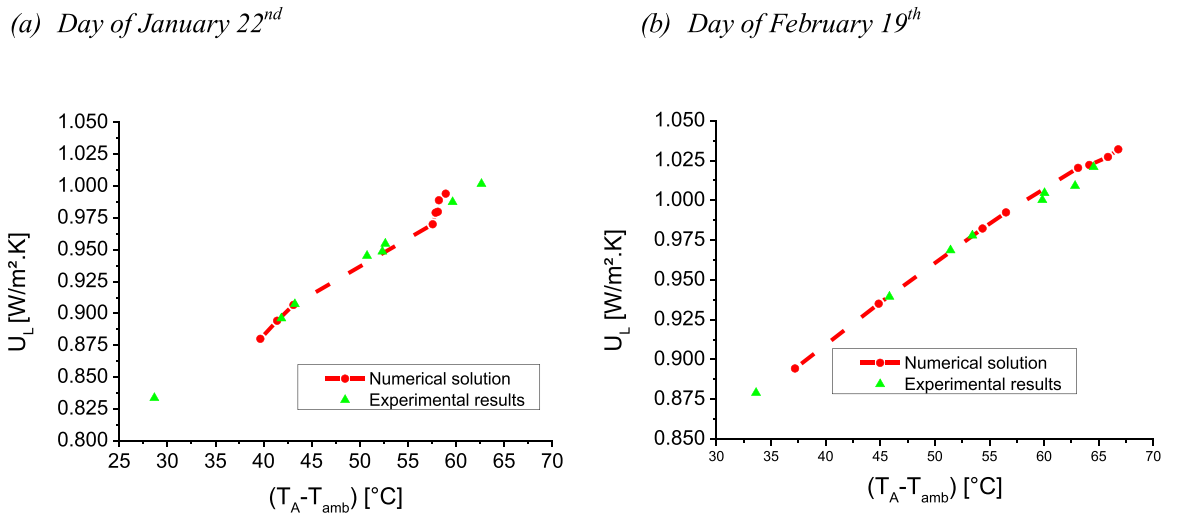

Fig. 8. Evolution of the thermal losses coefficient. (a) Day of January 22nd. (b) Day of February 19th.

- The temperature of the inlet water increases.
- The temperature of the absorber tubes increases.

Using an absorber tube with selective surface allows very significant reduction of these losses. In our case, the emissivity of our absorber tubes in the vicinity of 0.12, this value of emissivity could reduce greatly the thermal losses by radiation. In order to reduce heat loss, the transparent cover can be used around the absorber, because the transparent cover (glass tubes) is used to reduce convection losses between the absorber tubes and ambient air through the restraint of the stagnant air layer between the absorber tubes and the glass tubes. Also, it reduces radiation losses from the collector because the glass tubes are transparent to the shortwave radiation received by the sun, but it is nearly opaque to long-wave thermal radiation emitted by the absorber tubes (infrared greenhouse effect). the usage of glass tube around the absorber tubes in parabolic trough concentrator was used in a previous work [34,35,37]; this technique gives very good results, where the efficiency of the concentrator exceeded 60%.

There is another method to reduce losses by convection by creating vacuum (technique of suppressing convection) between the absorber tube and glass tube; where the vacuum envelope reduces convection and conduction losses between them.

Therefore, the correlation for the thermal loss coefficient of our prototype is given by:

- January 22nd, 2015

$$U_L = -7\times10^{-7}(T_A - T_{amb})^3 + 9\times10^{-5}(T_A - T_{amb})^2 + 0.001(T_A - T_{amb}) + 0.07458 \quad (28)$$

With a coefficient of determination (R^2) on the graph is equal to 0.9989.

- February 19th, 2015

$$U_L = -9\times10^{-7}(T_A - T_{amb})^3 + 10^{-4}(T_A - T_{amb})^2 + 0.0017(T_A - T_{amb}) + 0.07474 \quad (29)$$

With a coefficient of determination (R^2) on the graph is equal to 0.9978.

The Linear Fresnel reflector or more properly sense our solar water heating system produces the hot water using the sunlight as an energy source; this energy is available throughout the year. The hot water is required frequently to use in domestic uses (kitchen, bathroom, Swimming pools, etc.). The linear Fresnel concentrator is a device which supplies hot water, and that can complete the other types of solar water heaters (electricity, fossil fuels, etc.). The use of the linear Fresnel reflector as a solar water heating system is an economical, efficient and sustainable.

4. Conclusion

The linear Fresnel concentrator is a system that transforms solar energy into thermal energy. The primary aim of this paper was the validation of experimental results from a numerical simulation for the solar water heating system, where the linear Fresnel receiver as a device for thermal conversion. The performance of solar concentrator was evaluated in situ, where the tap water was used as a heat transfer fluid. The water is heated by the absorbed solar power that is transmitted by convection to the absorber tube.

The study was started with thermal modeling of the absorber tubes which was built on a very precise mathematical model; the model is based on the energy balance between absorber tubes and transfer fluid. The implicit finite difference method was used to discretize the governing equations of the phenomenon. A computer program was developed to control performance of the concentrator. The program is written in the MATLAB language.

The numerical results were compared with experimental results; it observed that the experimental and numerical results are convincing. The thermal efficiency of the concentrator exceeded 29%; the water temperature has reached up to 347 K, which the temperature range is low (at 60–80 °C). Results indicate that the performance of the solar reflector has a direct relationship with the direct solar radiation, the geometric and optical characteristics of a solar collector components and the climatic conditions of the site studied. The linear Fresnel reflector relies on solar energy, this latter can be used as solar water heating system; where the use of this device will solve many problems in many industrial of domestic areas.

Appendix A. Supplementary material

Supplementary data associated with this article can be found in the online version at http://dx.doi.org/10.1016/j.csite.2016.06.006.

References

[1] S.A. Kalogirou, Solar thermal collectors and applications, Prog. Energy Combust. Sci. 30 (2004) 231–295.
[2] A. Haberle, Linear fresnel collectors, in: Robert A. Meyers (Ed.), Encyclopedia of Sustainability Science and Technology, 2012, pp. 72–78, http://dx.doi.org/10.1007/978-1-4419-0851-3.
[3] F. Veynandt, Cogénération hélio thermodynamique avec concentrateur linéaire de Fresnel: modélisation de l'ensemble du procédé, in Institut National Polytechnique de Toulouse (INP Toulouse), Université de Toulouse, 2013, p. 213.
[4] C. Silvi, Italian contribution to CSP with flat reflectors, in: Presented at ISES Solar World Congress, 28 Aug.–02 Sept., Kassel, Germany, 2011.
[5] S.A. Kalogirou, Fresnel collectors, in: Solar Energy Engineering: Processes and Systems, 1st ed., Library of Congress Cataloging-in-Publication Data, 2009, p.152, ISBN 978-0-12-374501-9.
[6] P. Garcia, Outils d'évaluation technico-économique et d'aide à la conception des centrales solaires thermodynamiques du futur, in: Energétique et Environnement, Université de Perpignan, 2007, p. 35.
[7] B.S. Negi, S.S. Mathur, T.C. KAndpal, Optical and thermal performance evaluation of a linear Fresnel reflector solar concentrator, Sol. Wind Technol. 6 (1989) 589–593.
[8] Outils solaire, Centrales à réflecteurs de Fresnel, web: ⟨http://outilssolaires.com/developpement-durable/energie-solaire/reflecteurs-fresnel+a156.html⟩, 2012.
[9] C. Choudhury, H.K. Sehgal, A. Fresnel, Strip reflector-concentrator for tubular solar-energy collectors, Appl. Energy 23 (1986) 143–154.
[10] P.L. Singh, S. Ganesan, G.C. Yadav, Performance study of a linear Fresnel concentrating solar device, Renew. Energy 18 (1999) 409–416.
[11] D.R. Mills, G.L. Morrison, Compact linear Fresnel reflector solar thermal power plants, Sol. Energy 68 (2000) 263–283.
[12] P.L. Singh, R.M. Sarviya, J.L. Bhagoria, Thermal performance of linear Fresnel reflecting solar concentrator with trapezoidal cavity absorbers, Appl. Energy 87 (2010) 541–550.
[13] M.A. Moghimi, K.J. Craig, J.P. Meyer, A novel computational approach to combine the optical and thermal modelling of Linear Fresnel Collectors using the finite volume method, Sol. Energy 116 (2015) 407–427.
[14] M.A. Moghimi, K.J. Craig, J.P. Meyer, Optimization of a trapezoidal cavity absorber for the linear Fresnel reflector, Sol. Energy 119 (2015) 343–361.
[15] H.P. Garg, Design and performance of a large-size solar water heater, Sol. Energy 14 (1973) 303–312.
[16] Y.M. Dakhoul, R.E. Somers, R.D. Haynes, A conceptual design for a space-based solar water heater, Sol. Energy 44 (1990) 161–171.
[17] M. Hussain, T.P. Urmee, Design and fabrication of low cost solar water heaters, Renew. Energy (WREC) 9 (1996) 609–612.
[18] O. Helal, B. Chaouachi, S. Gabsi, Design and thermal performance of an ICS solar water heater based on three parabolic sections, Sol. Energy 85 (2011) 2421–2432.
[19] M. Arab, A. Abbas, Model-based design and analysis of heat pipe working fluid for optimal performance in a concentric evacuated tube solar water heater, Sol. Energy 94 (2013) 162–176.
[20] G. Gouhman, M. Koudrachova, N. Milevskaya, F. Eydinova, Surfaces sélectives: propriétés optiques et estimation de l'efficacité énergétique dans l'application aux récepteurs solaires, Phys. Appl. 15 (1980) 393–396.
[21] Bonnet, M. Alphilippe, P. Stouffs, Conversion thermodynamique de l'énergie solaire dans des installations de faible ou de moyenne puissance: Réflexion sur choix du meilleur degré de concentration, Rev. Energ. Ren.: presented at 11ème journée internationales de thermique, 2003, pp. 73–80.
[22] J.A. Duffie, W.A. Beckman, Solar Energy of Thermal Processes, 4th ed. John Wiley & Sons, 2013.
[23] Wikipedia, Déclinaison (astronomie), ⟨http://fr.wikipedia.org/wiki/D%C3%A9clinaison_%28astronomie%29⟩, Dernière modification le 25 Janvier, 2015.
[24] A.A. Sfeir, G. Guarracino, Ingénierie des systèmes solaires - Applications à l'habitat, Paris, 1981.
[25] J.D. Nixon, P.A. Davies, Cost-exergy optimisation of linear Fresnel reflectors, Sol. Energy 86 (2012) 147–156.
[26] Y.A. Cengel, Heat Transfer: A Practical Approach, 2nd ed., 2003.
[27] C. Tzivanidis, E. Bellos, D. Korres, K.A. Antonopoulos, G. Mitsopoulos, Thermal and optical efficiency investigation of a parabolic trough collector, Case Stud. Therm. Eng. 6 (2015) 226–237.
[28] Wikipedia, Reynolds Number, ⟨http://en.wikipedia.org/wiki/Reynolds_number⟩, 2015.
[29] Wikipedia, Prandtl Number, ⟨http://en.wikipedia.org/wiki/Prandtl_number⟩, 2014.
[30] Wikipedia, Viscosity, ⟨http://en.wikipedia.org/wiki/Viscosity#Kinematic_viscosity⟩, 2015.
[31] Wikipedia, Thermal Diffusivity, ⟨http://en.wikipedia.org/wiki/Thermal_diffusivity⟩, 2014.
[32] D.Y. Goswami, F. Kreith, J.F. Kreider, Off-normal incidence effects, in: Principles of Solar Engineering, 2nd ed., Taylor & Francis, 1999, 139.
[33] N.E. Gharbi, H. Derbal, S. Bouaichaoui, N. Said, A comparative study between parabolic trough collector and linear Fresnel reflector technologies, Energy Procedia 6 (2011) 565–572.
[34] M. Ghodbane, B. Boumeddane, S. Largot, N. Heniat, Simulation numérique d'un concentrateur cylindro-parabolique en el oued, Algérie, Int. J. Sci. Res. Eng. Technol. 3 (2015) 68–74.
[35] M. Ghodbane, B. Boumeddane, Numerical modeling of a parabolic trough solar collector at Bouzaréah, Algeria, Int. J. Chem. Petrol. Sci. 4 (2015) 11–25.
[36] M. Ghodbane, B. Boumeddane, N. Moummi, S. Largot, H. Berkane, Study and numerical simulation of solar system for air heating, J. Fundam. Appl. Sci. 8 (2016) 41–60.
[37] M. Ghodbane, B. Boumeddane, S. Largot, N. Heniat, Etude optique et thermique d'un concentrateur cylindro-parabolique en site d'Alger, Algerie, in: Presented at IXth International Congress on Renewable Energy and the Environment, Tunisia, 18–20 March, 2015.